INFLUENCE OF ALKALI METAL HYDROXIDES ON CORROSION OF Zr-BASED ALLOYS

Y.H. JEONG
Korea Atomic Energy Research Institute,
Dae Jun, Republic of Korea

H. RUHMANN, F. GARZAROLLI
Siemens-KWU, Power Generation Group,
Erlangen, Germany

Abstract

In this study the influence of group-1 alkali hydroxides on different zirconium based alloys has been evaluated. The experiments have been carried out in small stainless steel autoclaves at 350 °C in pressurized 17 MPa water, with in low (0.32 mmol), medium (4.3 mmol) and high (31.5 mmol) equimolar concentrations of Li-, Na-, K-, Rb- and Cs-Hydroxides. Two types of alloys have been investigated: Zr-Sn-(Transition metal) and Zr-Sn-Nb-(Transition metal). The corrosion behavior was evaluated from weight gain measurements. From the experiments the cation could be identified as the responsible species for zirconium alloy corrosion in alkalized water .The radius of the cation governs the corrosion behavior in the pre accelerated region of zircaloy corrosion. Incorporation of alkali cations into the zirconium oxide lattice is probably the mechanism which allows the corrosion enhancement for Li and Na and the significantly lower effect for the other bases. Nb containing alloys show lower corrosion resistance than alloys from the Zr-Sn-TRM system in all alkali solutions. Both types of alloys corrode significantly more in LiOH and NaOH than in the other alkali environments. Lowest corrosive aggressiveness has been found for CsOH followed by KOH. Concluding from the corrosion behavior in the different alkali environments and taking into account the tendency to promote accelerated corrosion, CsOH and KOH are possible alternate alkalis for PWR application.

INTRODUCTION

In order to maintain low corrosion and activation of corrosion products in pressurized light water reactors the primary water has to be pH controlled. This is performed usually by the addition of alkalizers such as lithium hydroxide or potassium hydroxide to the coolant. Under certain operation conditions with high operational temperatures locally increased void levels have to be anticipated. In out of pile loop experiments performed under heat flux conditions and in the presence of lithium hydroxide, enhanced corrosion of zircaloy cladding has been reported [1]. Even isothermal experiments performed in autoclaves in water under high pressure showed that lithium hydroxide is detrimental to the corrosion resistance of zircaloy.

Several studies using concentrations between 0.1 and 3 mol of LiOH in aqueous solutions have been performed in the past [2,, 3, 4, 5, 6]. Only few results are available from literature which include different alkalizers like sodium-, potassium- or other hydroxides from group I or II of the periodic table. Coriou et al. [7] investigated the influence of LiOH, NaOH, KOH and NH3 upon the corrosion in the temperature range of 330 to 370 °C. They found the highest effect on corrosion rate for LiOH and no effect for NH3. The threshold concentration for acceleration of corrosion was reported as 3 mmol for LiOH [14].

In the corrosive solution, in principle, either the cation or the OH-anion can induce enhanced corrosion. Some experimental results have been reported which should allow one to determine on the responsible ionic species for the enhanced LiOH corrosion. Hillner [4] reported no or only a slight increase of the corrosion for 1 molar Lithium nitrate (pH = 7.8). Perkins and Bush [8] measured a significant decrease in the aggressivness of the LiOH solutions if OH is converted to carbonate by exposure to air (pH decreased from 12.4 to 10.3). Furthermore, the addition of boric acid reduces the pH of the alkali solution and

also the corrosion aggressiveness [9, 10]. All these results can be interpreted that both the metal cation and the OH anion should have an significant effect on Zry corrosion in caustic solutions. No systematic study has been performed to decide this question or to investigate the influence of different alkali metals.

Mechanistic models have been suggested in the literature to explain the accelerating effect of LiOH [11]. The substitutional incorporation of Li+ into the growing zirconium oxide would cause an increased anion vacancy concentration which allows an accelerated charge transfer through the metal oxide interface and therefore enhanced corrosion. As pointed out recently by Cox [15] this incorporation model needs significantly effects on corrosion in the pretransition oxide if it should be valid.

A second mechanism which influences the morphology of the corrosion layer was addressed by Garzarolli et al. [12] to a modified crystal growth mechanism (crystallization of oxide) induced by alkalizers like LiOH. The influence the formation and conversion of primary growing tetragonal oxide nuclei to the monoclinic modification. As a result more equiaxed oxide grains than columnar structures are developed. Finally both mechanistic aspects are used by Ramasubramanian [11] who also indicated non dissociated LiOH as an responsible factor for the development of fast growing porous oxide layers on zirconium alloys.

Increased concentrations of Li in porous oxide structures under non isothermal, boiling conditions are responsible for the enhanced alkali induced corrosion of Zry (known as hideout [10]). This phenomenon suggests the diffusion of solute species in porous structures as a driving mechanism. Diffusion in aqueous solutions is governed by the radius of the solvated ion (under otherwise constant conditions). In the sequence of the group-I alkali cations Li^+ has the largest radius in opposition to Li+ in the crystal lattice (see Tab. 1). Therefore, if

Tab.1 Properties of Group-I alkali metals.

Metal	At.No	At.Wt %	Cryst. Struct.	Density (g/cm3)	At.Radius (pm)	Ion Radius pm (Coord.)	Ion Radius solv. (pm)	Ion Cond. 25 C (cm^2/ohm mol)	M.P (C°)	B.P (C°)
Li	3	6.94	BCC	0.53	152	76 (6)	340	38.7	186	1342
Na	11	23	BCC	0.968	185.8	102 (6)	276	50.1	97.7	881
K	19	39.1	BCC	0.86	227.2	151 (8)	232	73.5	63.6	756
Rb	37	85.5	BCC	1.52	247.5	161 (8)	228	77.8	39	686
Cs	55	133	BCC	1.89	265.5	174 (8)	228	77.2	28.45	678
Zr					159	72 (8)				
NH4						150 (6)		73.6		

an increased concentration of alkali is induced by a diffusion process in solution filled pores, the effect should be more pronounced for NaOH to CsOH in comparison to LiOH.

This study was performed without focusing on the mechanistic aspects of accelerated corrosion in alkalized environments. It was carried out in order to check the potential for alternate alkalizers in nuclear power plants. The influence of group-1 alkali hydroxides on two different types of zirconium based alloys was the objective of the investigation. Nevertheless, the study was designed in a way not to exclude mechanistic observations.

EXPERIMENTAL PROCEDURES

Critical evaluation of the literature shows a significant ambiguity between cation or anion influence on Zry corrosion in alkaline solutions. Therefore, a comparative experiment which should allow one to decide on the influence of the metallic ionic species must be performed at equimolar concentrations keeping the OH concentration constant. Experiments comparing effects in solutions with equal mass percentages (ppm) of hydroxides mean that different numbers of molecules are present in the reactive environment and therefore difficult to evaluate with respect to the active species. The range of applied concentrations in this study was chosen to cover the pure water condition (or at least the range of concentrations applied in PWRs (app. 2 ppm Li) up to concentrations above the threshold value reported for accelerated corrosion (30 ppm for LiOH) but avoiding concentrations which level out alloy composition sensitivities by being overly aggressive or bare the risk of crud deposition from the autoclave materials (1 mol of LiOH as reported by Ref.[15]).

The concentrations of Li-, Na-, K-, Rb-, and Cs-hydroxides selected for this study were 0.32 mmol, 4.3 mmol and 31.5 mmol, where 0.32 mmol (2.2 ppm Li) represents the standard concentration for lithium in the primary PWR coolant and 35.2 mmol (220 ppm Li) is above the threshold for accelerated corrosion for LiOH. The solutions were prepared from commercially available salts of analytical grade except for RbOH for which only a solution was available. Hydrates and noted impurities (carbonates) have been considered. Nevertheless, as can be seen from Table 2, some deviations from the intended equimolarity were revealed by chemical analysis of the solutions especially for RbOH and CsOH. The cation and anion concentrations have been analyzed independently. With the exception of RbOH, the cation- and anion concentrations are in fairly good agreement (accuracy of the OH determination +- 5 %). The Rb solution contained obviously much more carbonate than indicated. Identical stock solutions

Tab.2 Results of the chemical analysis of the used alkali solutions.

Alkali-	c(M+)	Molarity of M+, mmol			c(OH-	Molarity of OH-, mmol		
Hydroxide	ppm	Calculated	Measured	Dev.%	ppm	Calculated	Measured	Dev.%
LiOH	2.2	0.32	0.29	-9.4	5.3	0.31	0.3	-3.2
NaOH	7.2	0.32	0.29	-9.4	5.3	0.31	0.33	6.5
KOH	12	0.32	0.28	-12.5	5.3	0.31	0.35	12.9
RbOH	27	0.32	0.42	31.3	5.3	0.31	0.38	22.6
CsOH	42	0.32	0.38	18.8	5.3	0.31	0.4	29.0
LiOH	30	4.3	4.22	-1.9	73	4.3	4.3	0.0
NaOH	99	4.3	4.5	4.7	73	4.3	4.4	2.3
KOH	169	4.3	4.6	7.0	73	4.3	4.5	4.7
RbOH	369	4.3	5.6	30.2	73	4.3	4.8	11.6
CsOH	574	4.3	4.7	9.3	73	4.3	4.8	11.6
LiOH	220	31.5	31.7	0.6	535	31.5	32.5	3.2
NaOH	724	31.5	32.9	4.4	535	31.5	32.5	3.2
KOH	1231	31.5	32.6	3.5	535	31.5	34	7.9
RbOH	2692	31.5	44.9	42.5	535	31.5	35.5	12.7
CsOH	4186	31.5	33.8	7.3	535	31.5	34	7.9

were used for the corrosion experiments taking especially care not to expose them to CO_2 from the atmosphere to avoid changes in composition.

Corrosion tests have been carried out in small 100 ml static autoclaves at 350°C and 17 MPa. In order not to complicate the experiments, the temperature has been chosen far away from the critical temperature of water (374 °C). All samples were carefully kept submerged in the water during exposure. No special inert gas purging has been applied prior to closing the autoclaves. In comparable experiments no influence of remaining air was reported by Perkins [8]. Measurements of pH of the used solutions were performed. If pH values are compared before and after the 35 day run (Table 3) no significant differences for the higher alkali concentrations (4.3 mmol and 32.5 mmol solutions) can be observed. Only

Tab.3 Summary of pH measurements before and after the autoclave tests.

Alkali-Hydroxide	Molarity (mmol)	Cal.pH at 25°C	Measured pH at 25°C		
			Before Test	After 35d run	Diff.
LiOH	0.315	10.5	8.5	7	-1.5
	4.32	11.6	11.4	10.6	-0.8
	31.5	12.5	12.2	12.1	-0.1
NaOH	0.315	10.5	10	7.5	-2.5
	4.32	11.6	11.4	11	-0.4
	31.5	12.5	12.2	12.2	0
KOH	0.315	10.5	10.4	7.9	-2.5
	4.32	11.6	11.4	11.2	-0.2
	31.5	12.5	12.3	12.2	-0.1
RbOH	0.315	10.5	10	9.6	-0.4
	4.32	11.6	11.5	11.3	-0.2
	31.5	12.5	12.4	12.4	0
CsOH	0.315	10.5	10	7.8	-2.2
	4.32	11.6	11.5	11.2	-0.3
	31.5	12.5	12.4	12.4	0

Tab. 4 Composition of the test materials.

Alloy Type	Mark	Nb (%)	Sn (%)	Transition Metals* (TRM)
Zr-Sn-(TRM)	A-1	-	1,4	0,33
Group A	A-2	-	1,1	0,6
	A-3	-	0,8	0,8
Zr-Sn-Nb-(TRM)	B-1	0,3	0,8	0,5
Group B	B-2	0,8	0,8	0,3
	B-3	1.0	-	0,87

the low concentration 0.3 mmol Li-, Na-, K-, and Cs-alkali solutions lost their OH concentration during the run of the experiment.

Tested materials:

Two groups of Zr based materials were investigated. Table 4 gives the chemical composition of the alloys used for the corrosion test. The samples are grouped into

Group A : Zr-Sn-(Transition Metal) type

Group B : Zr-Sn-Nb-(Transition Metal) type.

The main interest was addressed to the influence of niobium under the experimental conditions. The samples were used in form of small (area app. 3 cm^2) flat material coupons or cladding tube segments (A1 and B3). The condition of the materials was mainly fully recrystallized. All samples have been pickled prior to testing. Corrosion behavior was evaluated from the weight gain. The oxides formed in various alkali hydroxides were investigated by metallograpy and some of them characterized by SEM.

3. RESULTS

3.1. Influence of alloy composition under different alkali environments.

The weight gains measured for the different alloys up to 150 day exposures under various alkali environments are compiled in Table 5. Fig.1 to 5 show graphical presentations of the findings for the materials in low concentration (0.31 mmol, top diagram) medium concentration (4.3 mmol, middle diagram) and high concentration (32.5 mmol, bottom diagram) of Li-, Na-, K-, Rb- and Cs-hydroxide solutions, respectively.

Low concentration behavior:

As shown in Fig.1 to 5 in the LiOH test, group A alloys had low weight gains (around 30 mg/dm^2) in the pre-transition region after 150 day exposure time without any significant acceleration of corrosion rate. However the Nb-containing alloys (group B) exhibits generally higher corrosion rate than group A alloys if the Nb concentration is above 0.3 % (B2 and B3). The low Nb B1 alloy behaves very similar to Zr-Sn-(TRM) materials. The corrosion behavior in low concentration of NaOH, KOH and CsOH solution (Fig.2, 3 and 5) is not very different from that in LiOH. In RbOH solution (Fig.4) group B alloys showed somewhat higher weight gains and corrosion rates than in other alkali solutions. This result may be induced by the deviations in the Rb concentrations in solution. As can be seen from the data of chemical analysis (Table 2), the difference between cation and anion concentration is high for the RbOH solution. This higher corrosion in Rb is also visible at higher alkali concentrations and is not eliminated by correction to the nominal concentration what would point to a higher sensitivity of Nb alloys to Rb^+. The carbonate concentration has not been

Tab. 5 Corrosion Results.

Alloy	conc. MOH (mmol)	Exposure (day)	Weight Gain (mg/dm²)				
			LiOH	NaOH	KOH	RbOH	CsOH
A1	0,315	90	24,1	24,1	25,1	28,8	26,2
		120	26,9	27,0	27,3	31,5	29,6
		150	31,1	29,2	28,9	32,4	31,2
	4,3	90	25,5	24,3	23,7	30,3	25,4
		120	29,0	27,3	27,1	36,1	28,4
		150	31,2	28,0	27,4	39,4	29,9
	31,5	90	182,0	28,1	25,0	29,7	25,6
		120	630,0	30,8	28,1	31,1	28,0
		150	906,0	47,0	31,0	34,2	29,4
A2	0,315	90	22,7	22,3	22,3	25,6	25,0
		120	24,3	24,5	25,3	27,5	25,8
		150	27,0	27,7	26,3	28,8	27,8
	4,3	90	24,1	23,6	22,5	26,5	21,7
		120	26,3	26,8	25,5	32,2	24,0
		150	28,7	27,6	24,9	35,8	25,4
	31,5	90	40,2	27,2	23,5	24,6	21,6
		120	109,0	28,0	26,3	28,0	24,0
		150	237,0	29,4	27,6	28,6	25,0
A3	0,315	90	23,3	23,8	23,6	26,1	28,1
		120	26,1	25,5	26,2	29,0	28,6
		150	29,9	28,4	26,3	30,1	31,7
	4,3	90	27,2	29,6	23,8	29,0	23,6
		120	30,7	31,8	26,2	35,5	26,8
		150	34,9	33,0	26,7	38,4	28,2
	31,5	90	565,0	29,6	27,5	26,9	24,3
		120	1130,0	30,5	29,5	28,7	26,8
		150	1548,0	31,7	29,9	30,7	28,3
B1	0,315	90	25,1	22,9	23,4	26,6	26,7
		120	26,4	25,9	27,1	31,4	28,3
		150	30,2	29,5	29,1	34,2	32,0
	4,3	90	26,7	24,0	22,8	31,0	23,2
		120	32,4	26,7	27,3	40,0	26,5
		150	39,1	28,5	27,5	45,9	28,6
	31,5	90	1307,0	27,5	26,2	27,9	23,5
		120	1992,0	29,7	29,4	31,6	26,3
		150	2462,0	32,8	31,2	34,1	28,1
B2	0,315	90	46,3	57,4	65,4	87,0	66,2
		120	65,1	71,6	84,0	111,0	83,0
		150	81,7	84,6	96,2	132,0	96,7
	4,3	90	63,1	47,6	42,8	75,7	32,0
		120	102,0	67,6	57,2	108,0	38,0
		150	108,0	89,4	71,2	130,0	44,1
	31,5	90	235,0	46,9	49,2	52,1	38,4
		120	919,0	52,3	56,8	61,1	42,7
		150	1499,0	61,8	64,2	71,3	47,8
B3	0,315	90	37,1	38,4	43,0	72,1	41,4
		120	43,7	47,7	52,7	98,1	51,9
		150	51,9	62,6	65,0	128,0	65,2
	4,3	90	80,8	49,5	46,5	97,0	36,3
		120	140,0	72,9	57,0	138,0	41,6
		150	155,0	93,0	119,0	188,0	46,7
	31,5	90	3203,0	-1478,0	-322,0	-245,0	-26,0
		120	4300,0	-2400,0	-550,0	-480,0	-185,0
		150	4600,0	-2974,0	-713,0	-632,0	-315,0

Negative values indicate spalling.

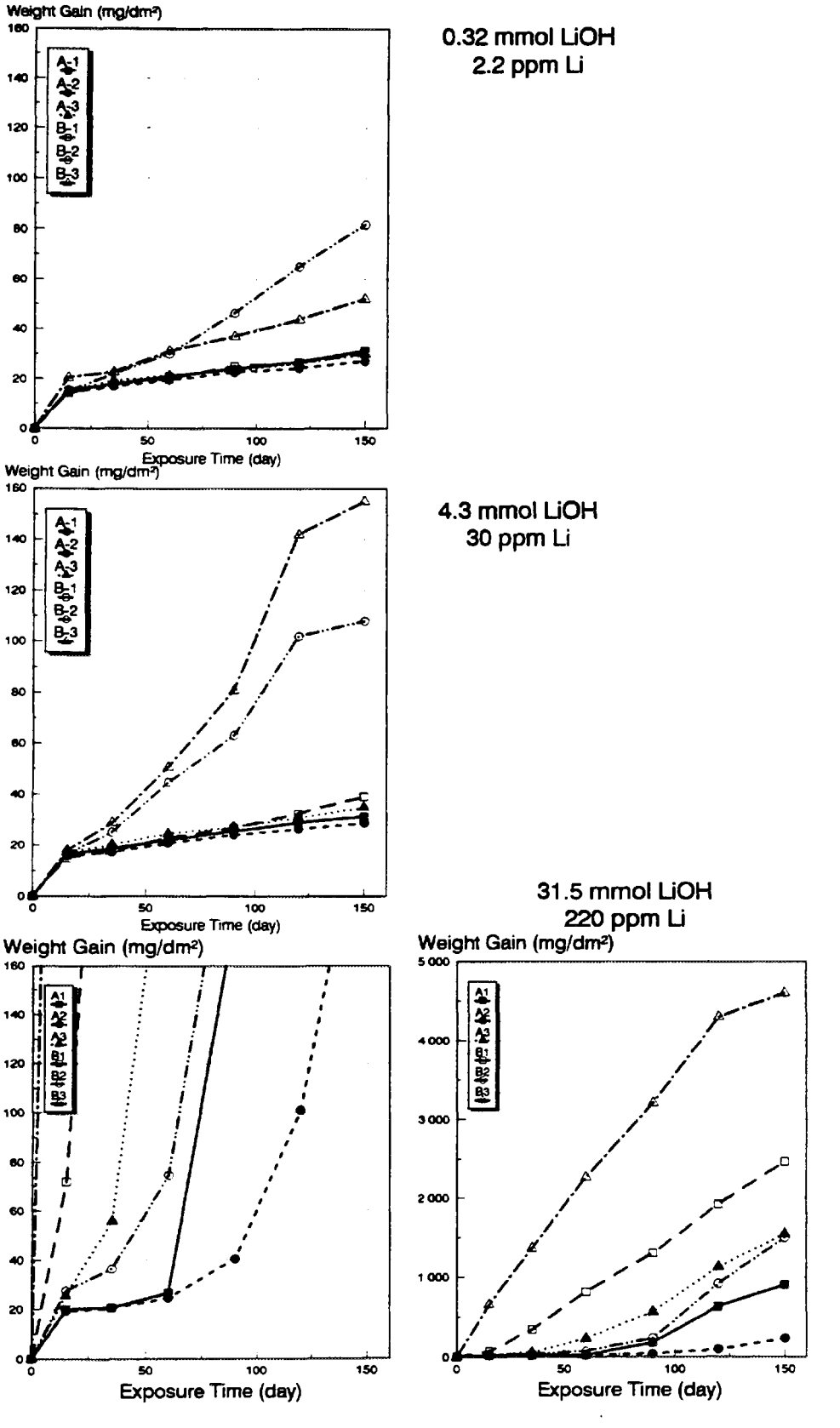

Fig. 1 Corrosion of different Zr alloys in LiOH. Test conditions: 350 °C, 17 MPa. Weight gain vs. exposure time

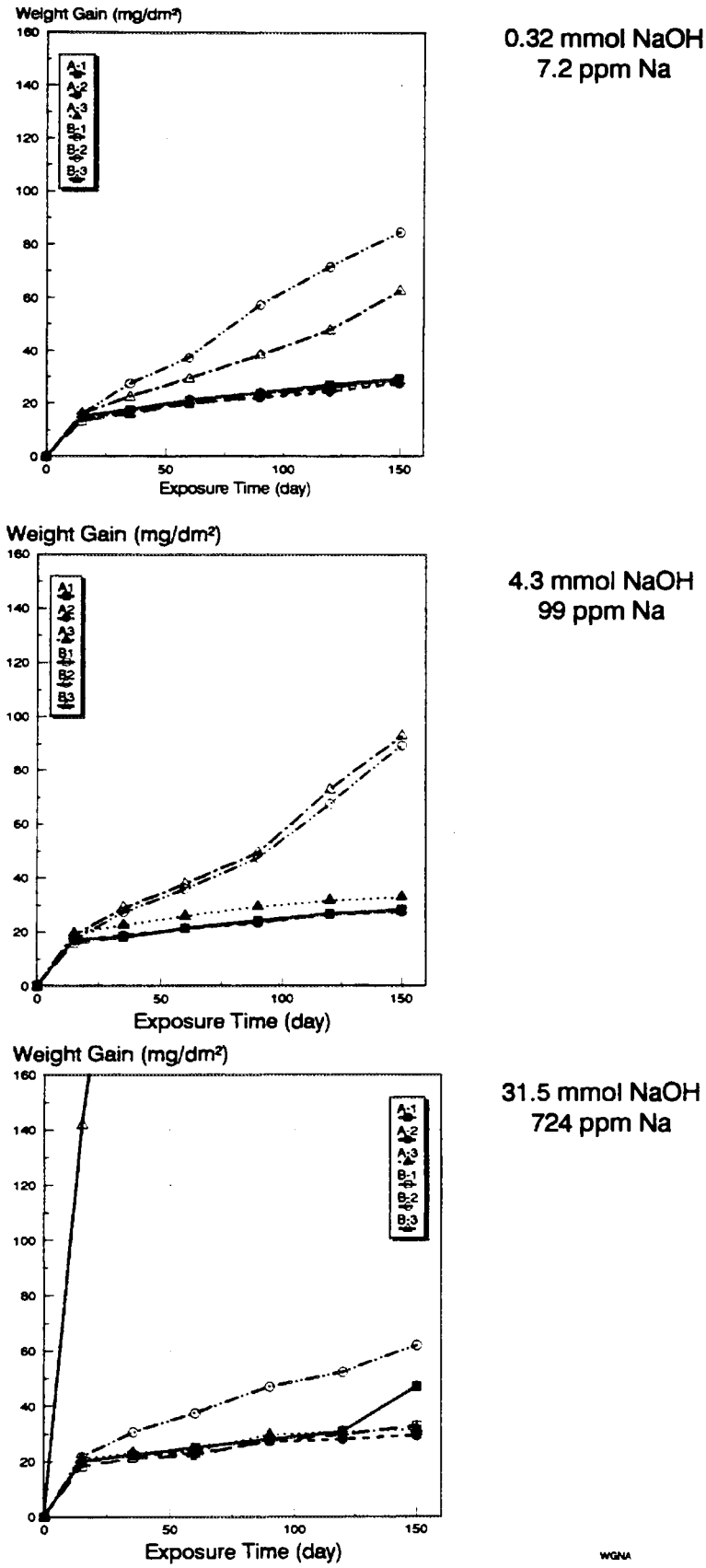

Fig. 2 Corrosion of different Zr alloys in NaOH. Test conditions: 350 °C, 17 MPa. Weight gain vs. exposure time

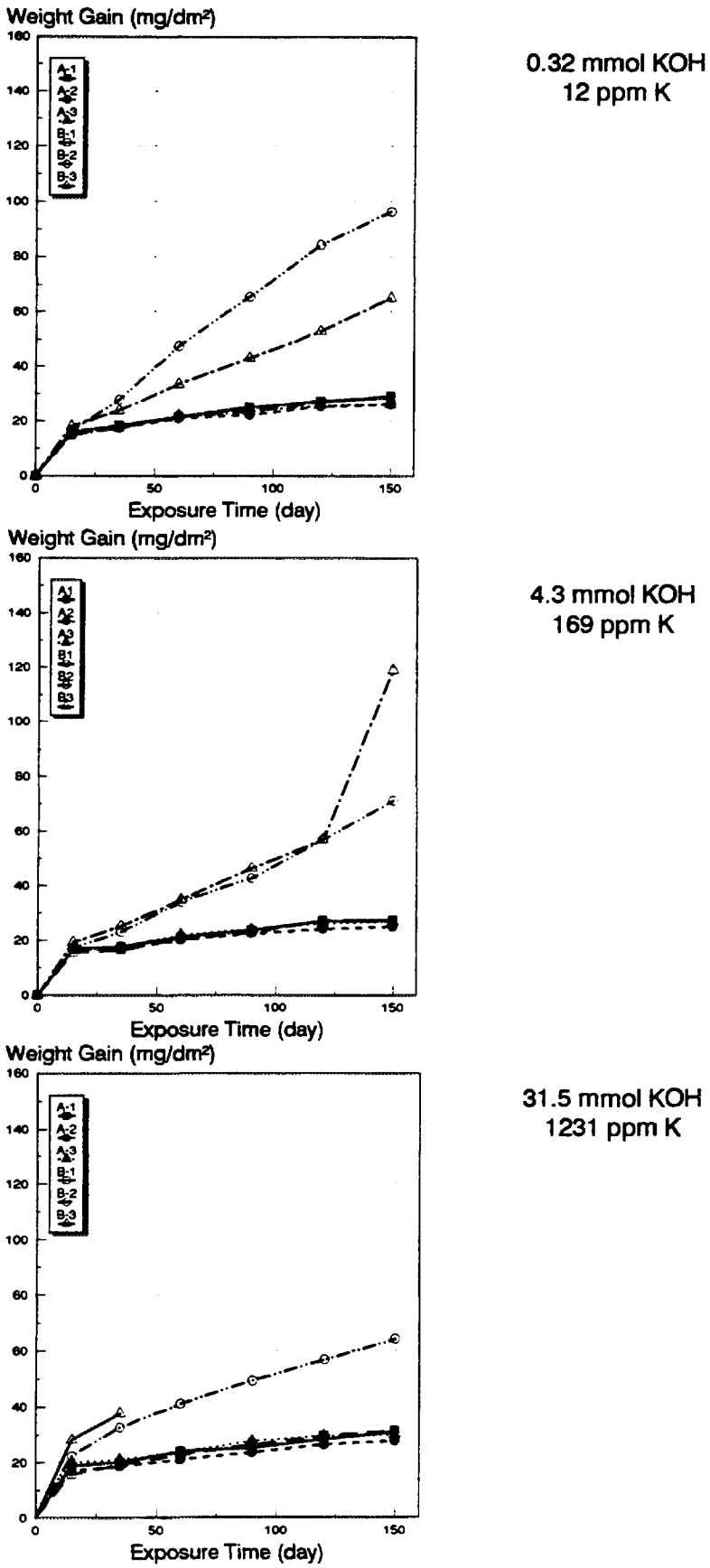

Fig. 3 Corrosion of different Zr alloys in KOH. Test conditions: 350 °C, 17 MPa. Weight gain vs. exposure time

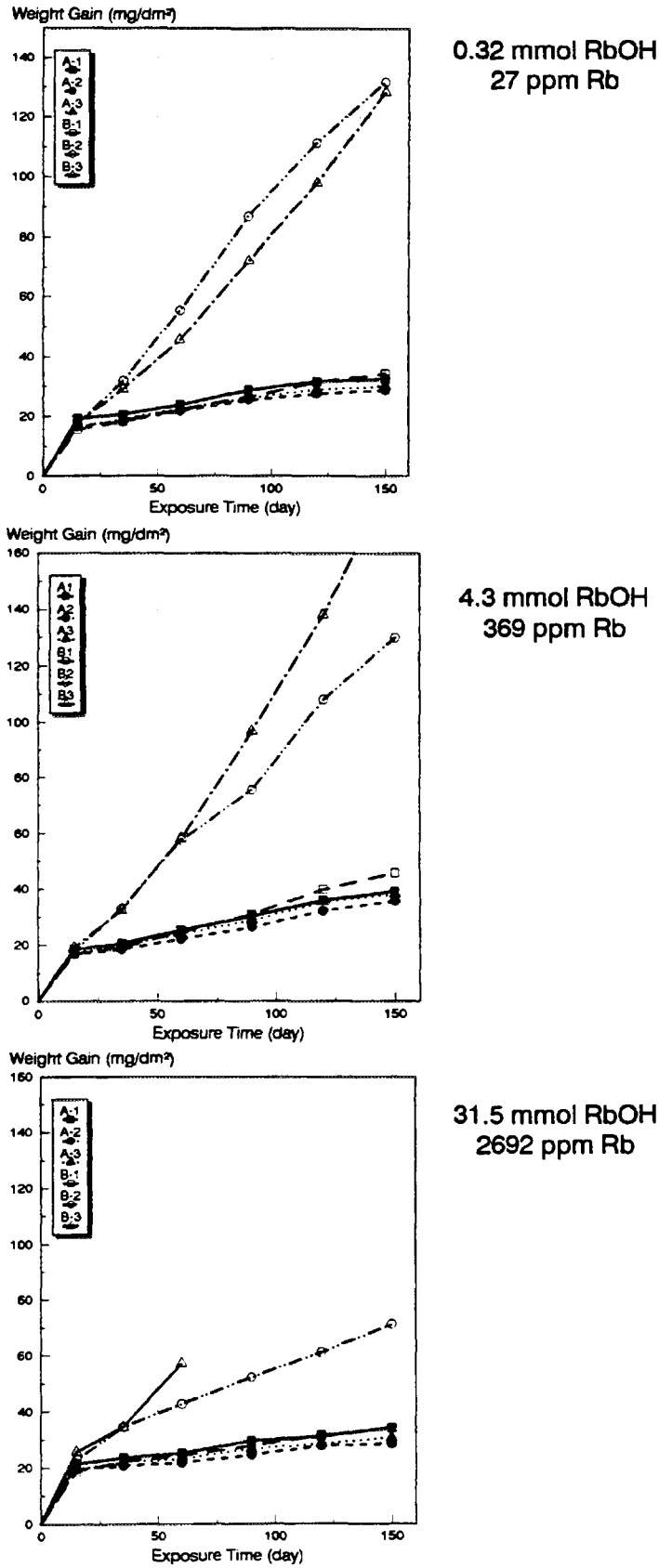

Fig. 4 Corrosion of different Zr alloys in RbOH. Test conditions: 350 °C, 17 MPa. Weight gain vs. exposure time

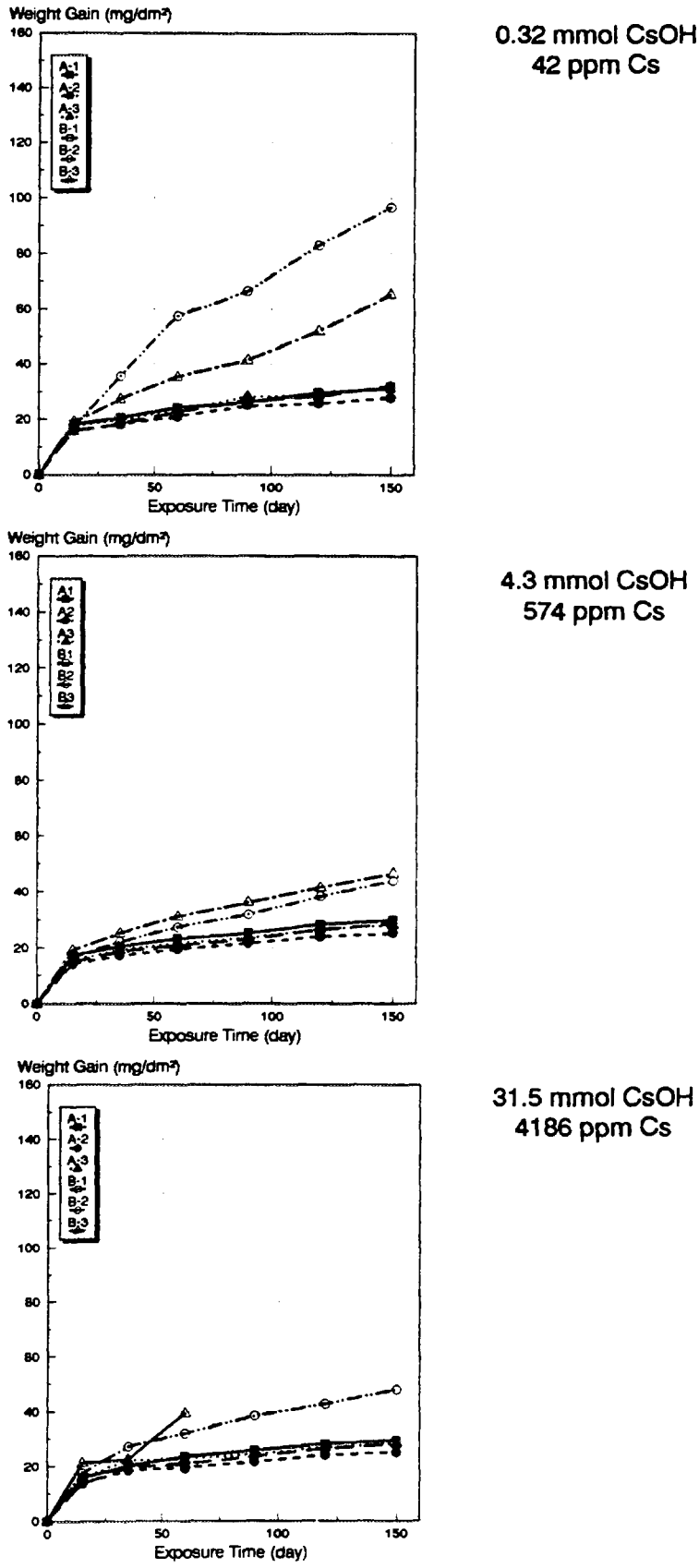

Fig. 5 Corrosion of different Zr alloys in CsOH. Test conditions: 350 °C, 17 MPa. Weight gain vs. exposure time

determined but may be responsible for the effect. A detrimental influence of carbonate anions on the corrosion of Nb alloys was reported by Ref. [16].

Medium concentration behavior:

The middle diagrams of Fig.1 to 5 show the corrosion behaviors of the test materials under medium concentrations (4.3 mmol) of Li-, Na-, K-, Rb- and Cs-hydroxides, respectively. The ranking between group A and B materials keeps similar. B3 within group B alloys now shows the highest weight gains of all tested materials. B3 alloy is the only material which shows in 4.3 mmol KOH an onset to post transition accelerated corrosion. Corrosion in 4.3 mmol Rb solution (Fig. 4 middle) is characterized by somewhat higher corrosion rates for B2 and B3 materials comparable to the behavior in LiOH. The group A samples show minor, but significant variations in weight gains what will be analyzed in detail later.

High concentration behavior:

The lower diagrams in Fig.1 to 5 present corrosion results in high concentration (31.5 mmol) alkali hydroxides. In LiOH all samples show enhanced or accelerated corrosion after 150 day exposure. The onset of acceleration and the corrosion rate depends significantly on alloy composition as can be seen in the diagram with extented weight gain scale in Fig. 5. The decrease of the corrosion rate of B-3 alloy after 120 day may be caused by oxide spalling. Generally group A alloys behave better than group B alloys. A2 alloy among the all samples tested has the best corrosion resistance in high concentration LiOH solution .

The high concentration behavior of the materials in Na, K, Rb and Cs solutions are very similar. Weight gains keep below 50 mg/dm² for group A

alloys. A1 alloy in 32.5 mmol NaOH may be starting starting to experience corrosion enhancement. From the group B alloys B3 experienced spalling in all alkali solutions except LiOH. On B3 corrosion layers grown in Na, K, Rb and Cs solution spalled off at low weight gains and short exposure times. The reason for this observation is found in different morphologies of the corrosion layers formed in LiOH in comparison to the other alkali solutions. This was confirmed by a SEM investigation comparing LiOH and NaOH grown corrosion layers of sample B3 as shown in Fig. 7. The back scatter electron images show cross sections of sample B3 approximately at the same distance from the metal oxide interface at the same magnification. Both oxides are structured by horizontal pores but in the case of the NaOH grown corrosion layer coarser grains and extensive separation of layers is visible.

3.2 Influence of the different hydroxides on corrosion

The influence of the different alkali hydroxides on one alloy representing group A and group B will be discussed in this section. For this reason in Fig. 8 and Fig. 9 weight gains obtained in the different alkali environments after 90, 120 and 150 day exposure are plotted. The values are linearly corrected according to the deviations from the target concentrations of the alkali solutions revealed by chemical analysis (Table 2). The x-scale represents the alkali hydroxide by the cation radius of the alkali metal (see Table 1). The ion radii used for the plots are those for the highest coordination (6 in the case of Li and Na, 8 for K to Cs). This is reasonable due to the fact that if an alkali cation is incorporated into the zirconia lattice substituting a zirconium 4^+ cation it would be surrounded by 8 oxide anions in the cubic modification fluorite lattice). In the monoclinic modification Zr^{4+} is surrounded by 7 nearest oxygen neigbours as determined by structure

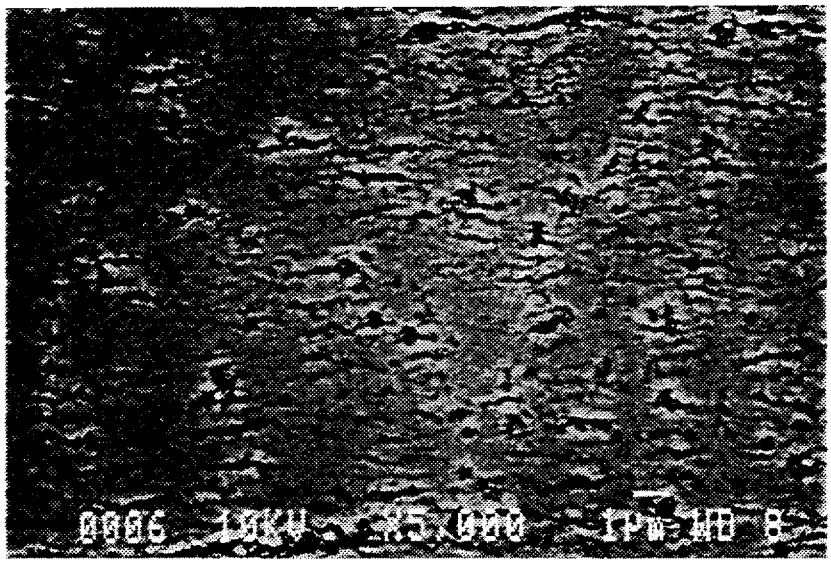

LiOH

Magnification: V = 5000 : 1

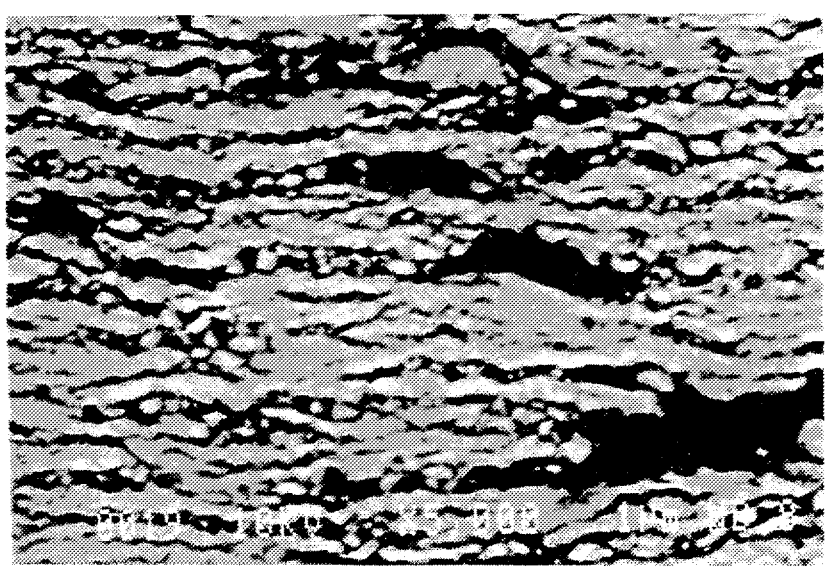

NaOH
(spalled)

Magnification: V = 5000 : 1

Test Conditions: 350 °C, 17 MPa, Alkali Concentration 31.5 mmol, Exposure 90 d.

Fig. 6 Microstructure of corrosion layers of sample B3 in LiOH and NaOH. SEM investigation (back scatter electron mode) .

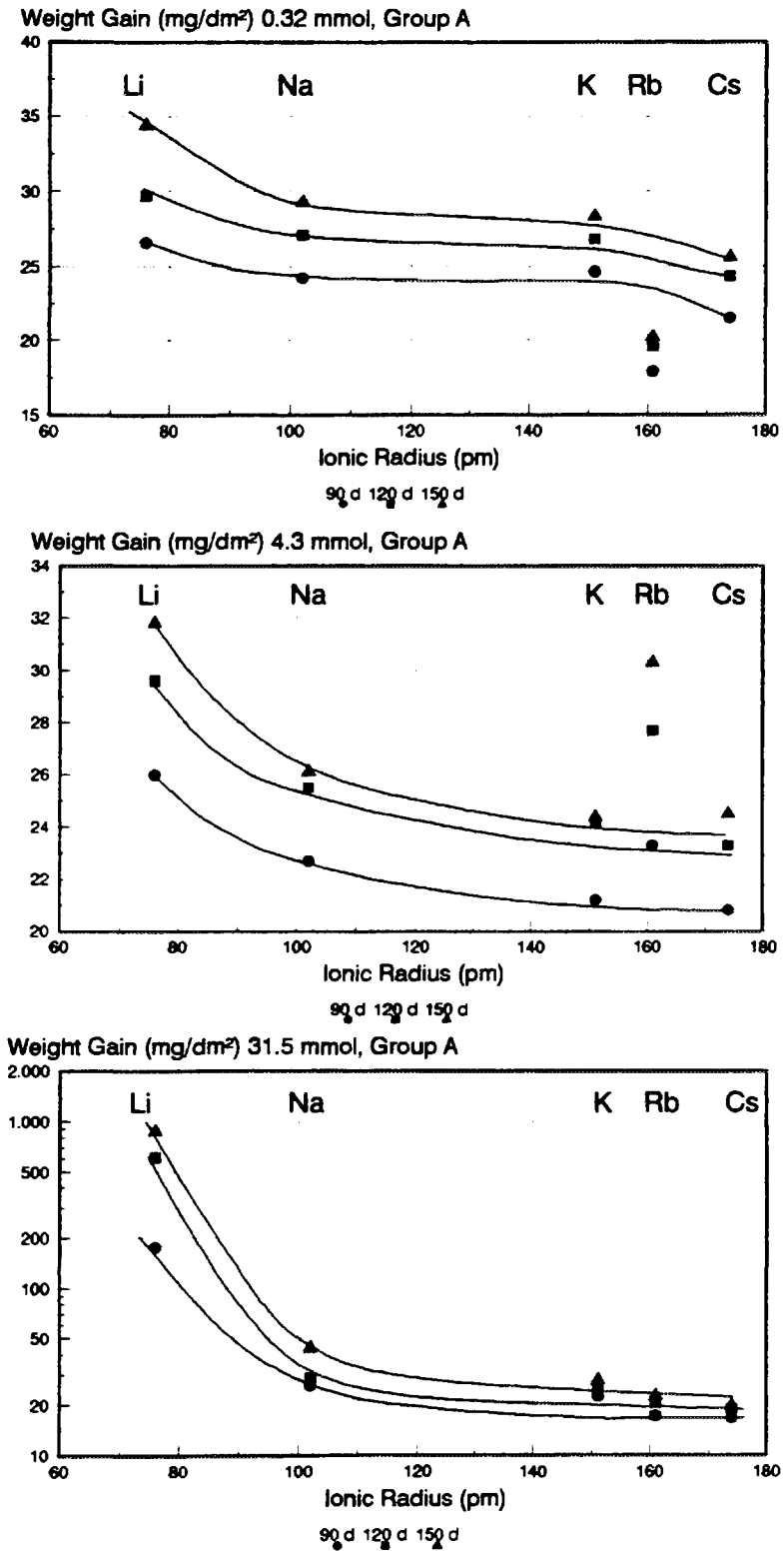

Fig. 7 Comparison of the corrosion behavior of group A materials (Zr-Sn-TRM) in different alkali hydroxide environments.

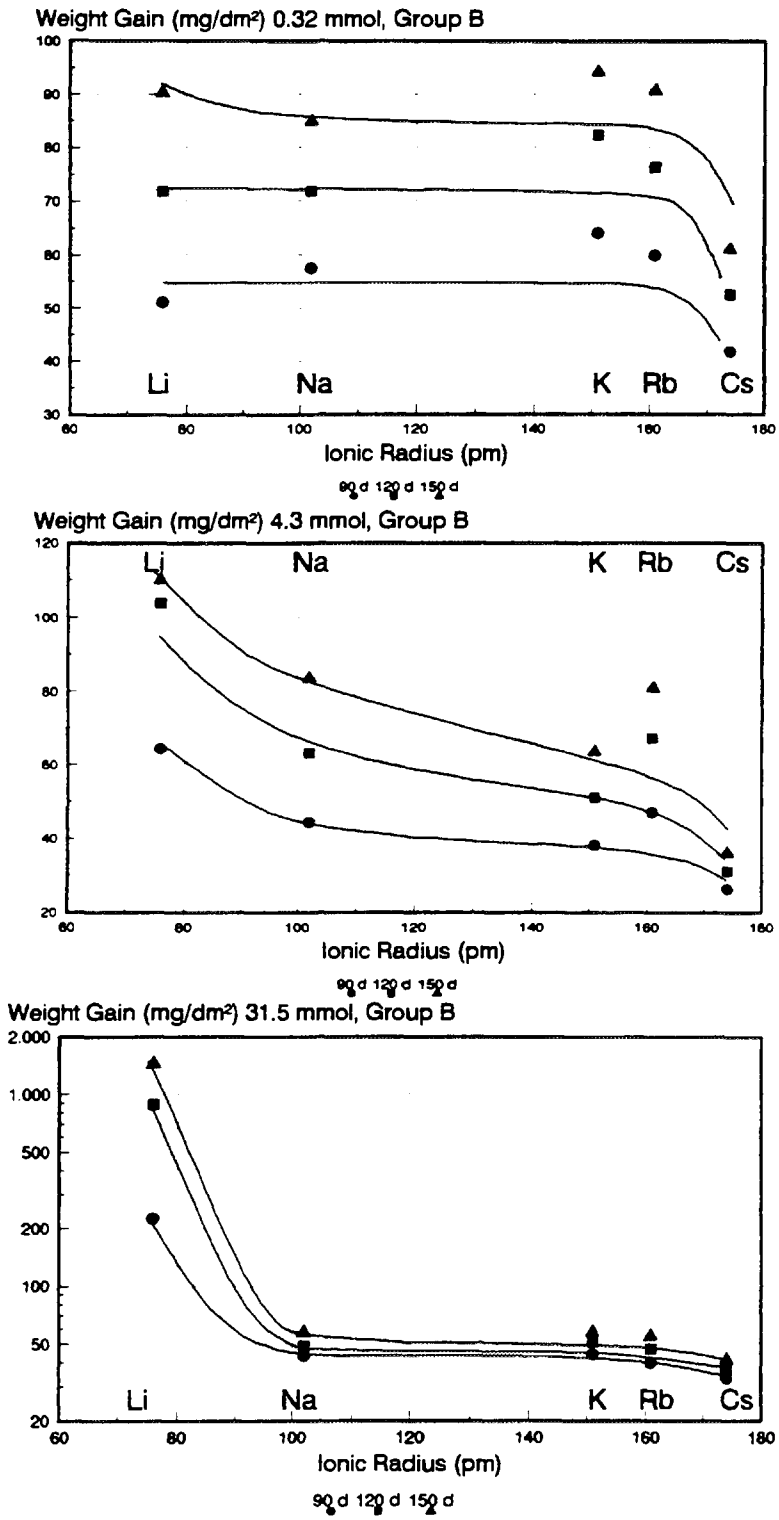

Fig. 8 Comparison of the corrosion behavior of group B materials (Zr-Sn-Nb-TRM) in different alkali hydroxide environments.

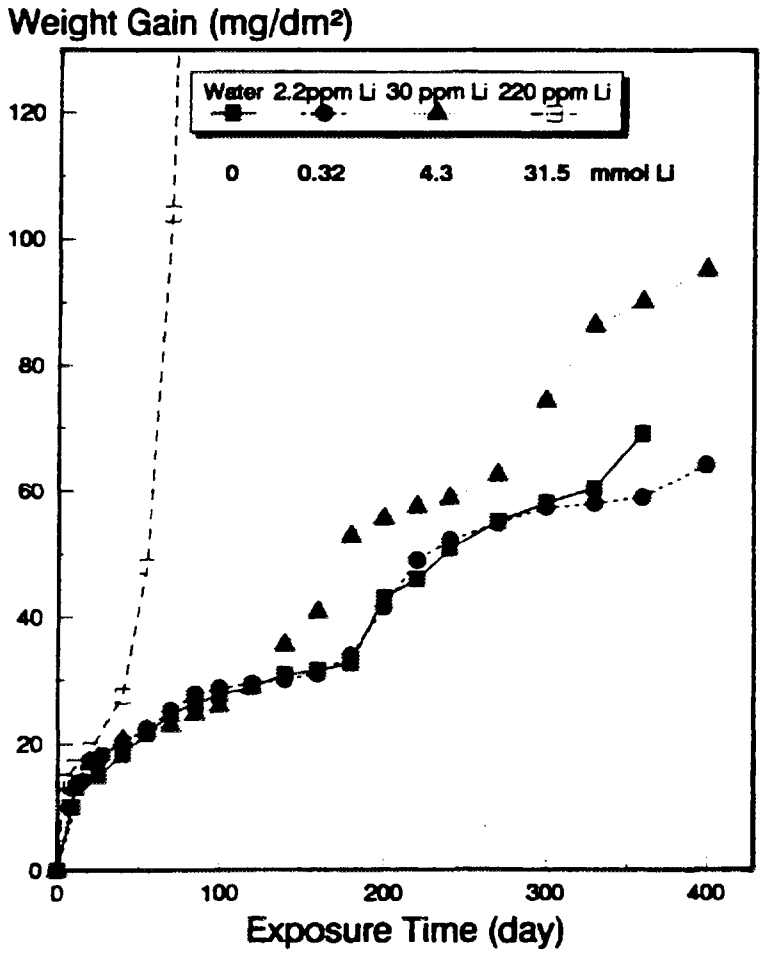

Fig. 9 Long term corrosion behavior of sample A1 in LiOH solutions of different concentrations. Test conditions: 350 °C, 17 MPa water.

analysis [17]. The figures compile weight gain data for the three hydroxide concentrations applied in this study.

On the first glance the general tendency observed is a more or less continuous decrease of weight gain with increasing ion radius of the alkali metal. No big alloy depending differences in this behaviour can be seen between group A (represented by A1 alloy) and group B materials (represented by B2 alloy) except of the range of weight gains covered. The Rb data at low and medium concentration do not follow the general trend. This may indicate additional influencing ionic species in these solutions.

3.3 Influence of alkali hydroxide concentration

The corrosion results reported in Fig. 1 to 5 showed a strong dependency of corrosion on the concentration of the applied solution. Especially, the point of onset for enhanced corrosion depends on concentration. The effect of accelerated corrosion in LiOH has been reported earlier and was recently reconfirmed [13]. In Fig. 10 and 11 long term exposure results are shown for sample A1 and A2, respectively. Two different regions can be distinguished in the weight gain curves: An enhanced corrosion significant for Li concentrations above 4.3 mmol (30 ppm) and accelerated corrosion for Li concentrations above 31.5 mmol (220 ppm). The onset of enhanced

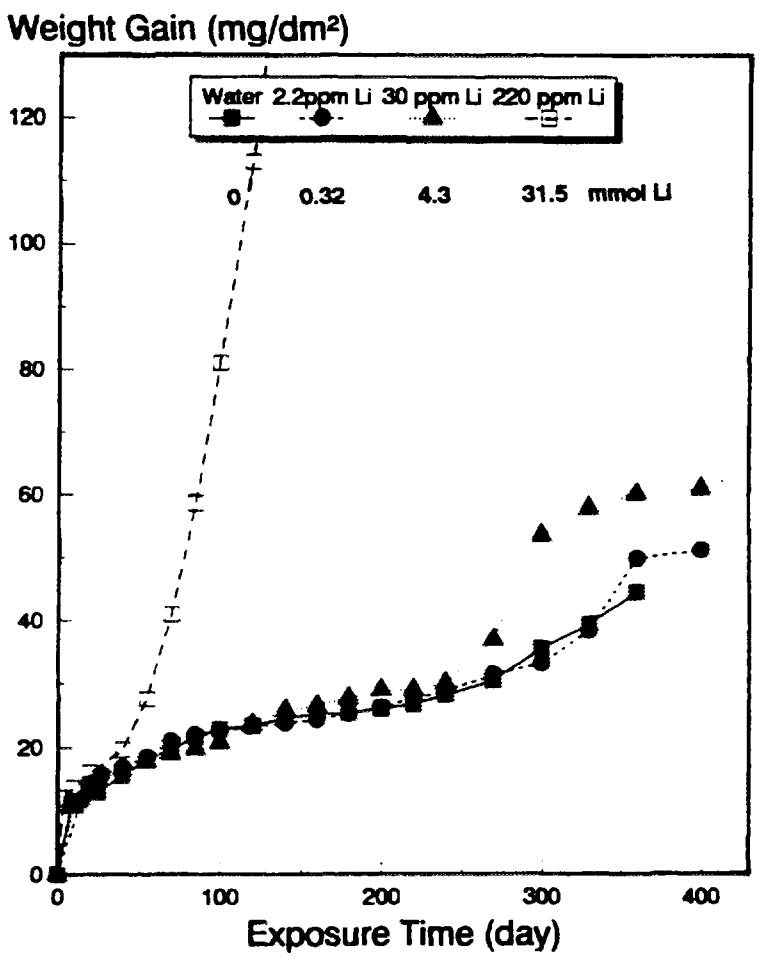

Fig. 10 Long term corrosion behavior of sample A2 in LiOH solutions of different concentrations. Test conditions: 350 °C, 17 MPa water.

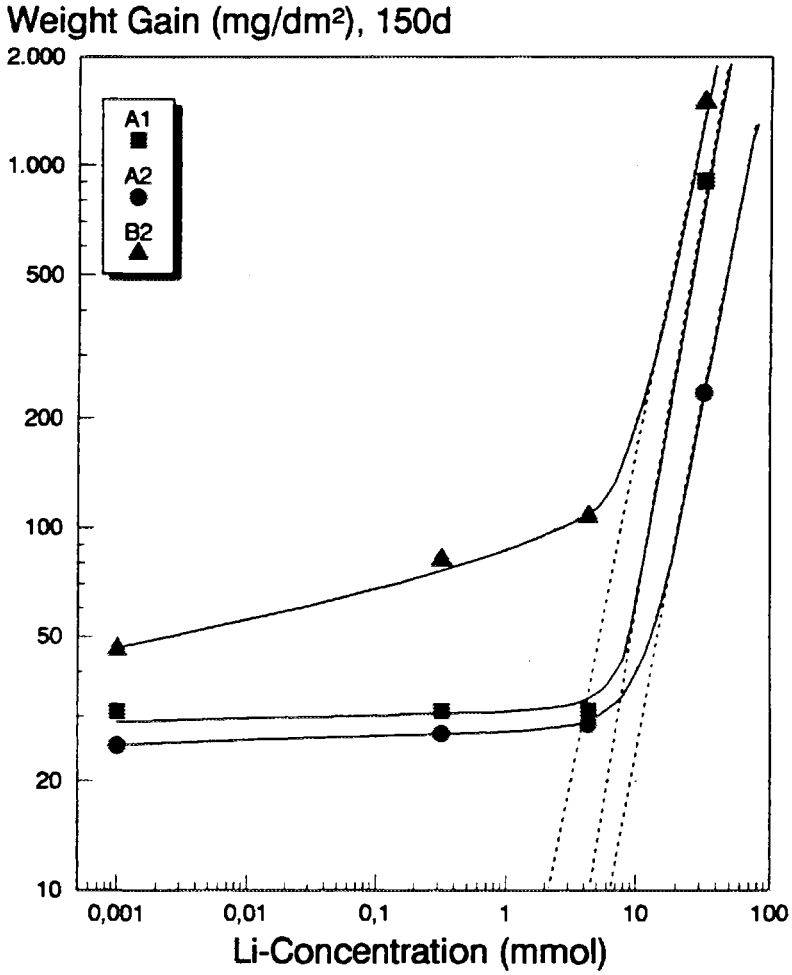

Fig. 11 Variation of weight gain as function of Li-content. Test conditions: 350 °C, 17 MPa water.

corrosion (which corresponds to the first transition in water tests) is sensitive to the alloy composition. Obviously the weight gain at this point is not strongly influenced and increases more or less constantly with increasing Li concentration. Even for Li enhanced corrosion at 32.5 mmol, differences in the corrosion rate for the different materials are still visible. But it should be noted that experiments with even higher alkali concentration showed an increasing lost of differentiation with respect to alloy composition. The onset of Li induced increased corrosion can be deduced from Fig. 11. For sample A1 and A2 extrapolation gives values around 10 mmol (70 ppm Li); for alloy B2 with poor corrosion behavior a value below 10 mmol is obtained. These values for the onset of an Li

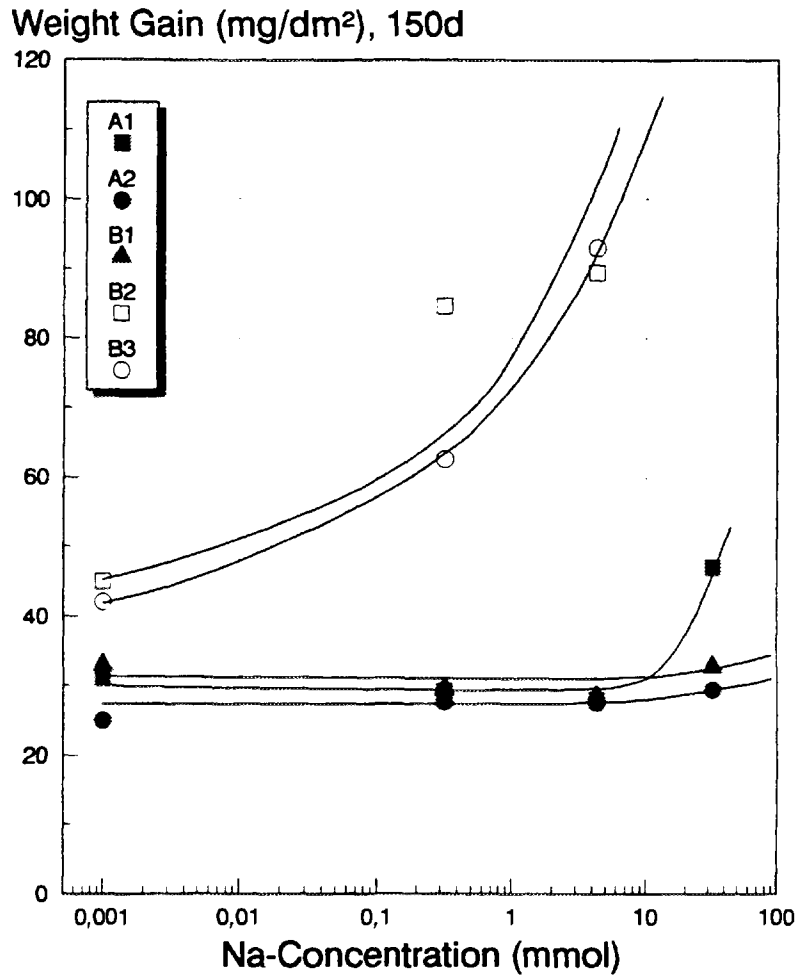

Fig. 12 Variation of weight gain as function of Na-content. Test conditions: 350 °C, 17 MPa water.

induced enhanced corrosion are somewhat lower but within the range of values reported by other authors [4, 9, 14].

Different behavior is found for corrosion in the other solutions. From group A materials only A1 showed an increase of corrosion at the highest NaOH concentration applied in the test (Fig. 13). For the other alloys or solutions no enhanced corrosion can be observed. The behavior of niobium alloys (group B samples) is different. B1 behaves like Group A materials without increase of corrosion. B3 and B2 corrosion is enhanced in NaOH already at lowest concentrations. At the highest alkali concentration B2 exhibits a decrease of weight gain in all solutions except LiOH.

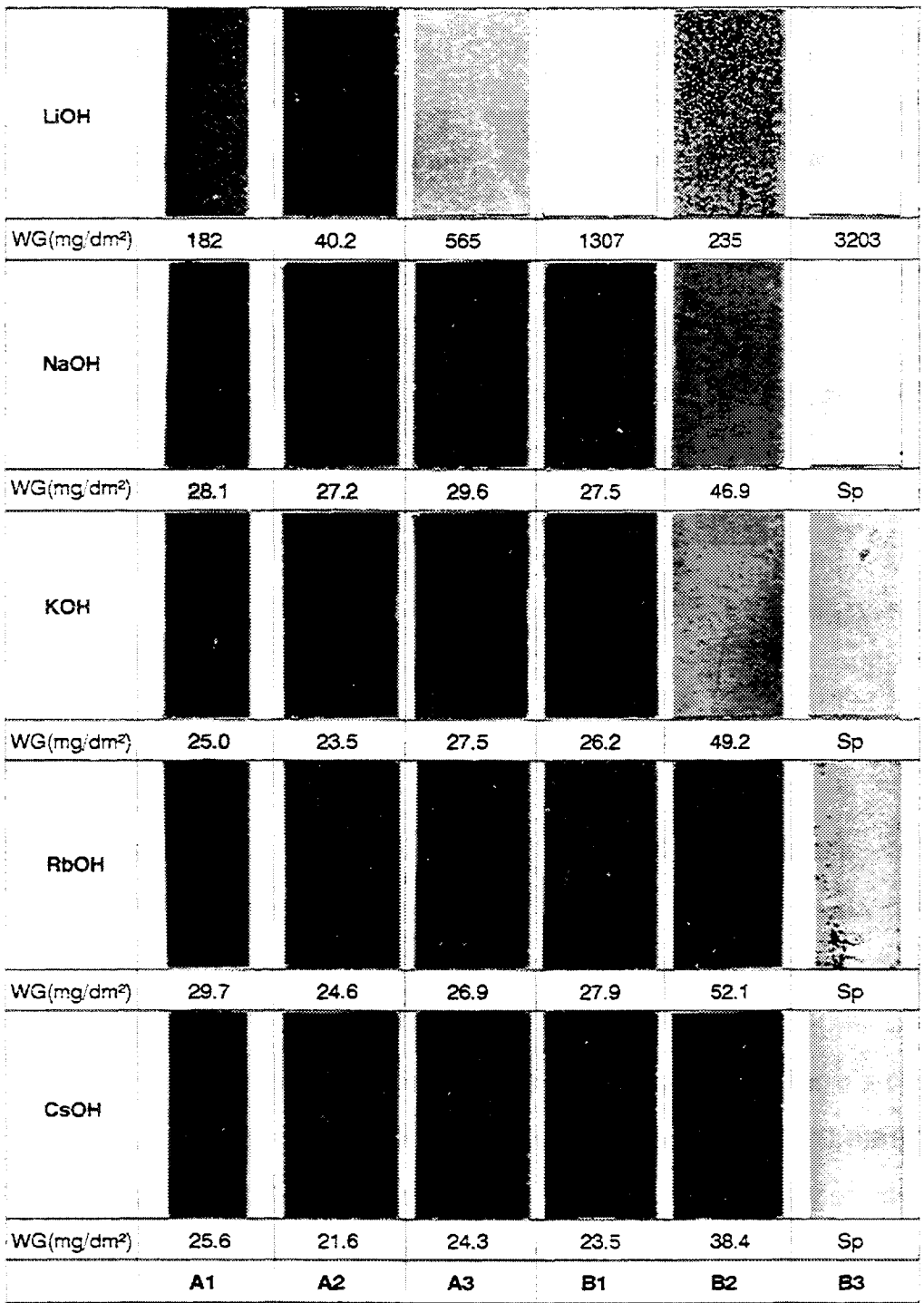

Fig. 13 Surface appearance of samples exposed to 31.5 mmol alkali hydroxide solutions for 90 days. Test condition: 350 °C, 170 MPa water.

3.4 Visual Appearance and Microstructures of oxides

Fig. 13 shows the surface appearance of the samples exposed to 31.5 mmol alkali hydroxides for 90 day at 350°C. The oxides formed in LiOH solution show a different surface appearance depending on alloy composition. Black oxide is found for A-2, gray oxide for B-3, B-1 and A-1, and nodular oxide for A-1 and B-2. In other alkali solutions (Na, K, Rb and Cs hydroxides) most alloys showed the black oxide only sample B-3 appears gray or white with spalling of oxide. This results are consistent to the variation of weight gain shown in Fig.1 to Fig. 5.

4. DISCUSSION

4.1 Influence of alloy composition

The results presented show a significant difference in the behavior of Zr-Sn-(Transition Metals, TRM) and Zr-Nb-(TRM) alloys. In group B, alloys containing Nb below 0.3 % are comparable in their corrosion resistance to Zr-Sn-(TRM) materials. Under the test conditions, Nb containing alloys showed a significantly higher corrosion rate in all alkali solutions. Accelerated corrosion occurred in LiOH and for the samples with low corrosion resistance also in NaOH, KOH, and RbOH. The corrosion behavior of the high Nb alloy in RbOH is comparable to that in LiOH, but the structures of the corrosion layers developed are different. No tendency toward spalling is observed only for LiOH grown oxides in contrast to all other alkali environments.

Zr-Sn-(TRM)-alloys show accelerated corrosion only in LiOH and for one material (A1) just beginning after 120 day exposure in NaOH. In all other

alkali solutions no acceleration is observed. The weight gains developed up to 150 days are below 50 mg/dm². A detailed analysis shows dependencies in different alkali hydroxides which can be understood by Zr substitution in the oxide lattice of this pre transition oxides. In LiOH a remarkable differentiation for the different alloy compositions is visible at concentrations above 4.3 mmol up to 31.5 mmol.

Comparing the tendency to undergo accelerated corrosion for different materials in different alkali solutions NaOH would be not the first choice as a substitute alkali due to acceleration found for niobium alloys. Lowest corrosion enhancement is observed for CsOH. From this study we would not recommend to use RbOH but KOH seems to be a good compromize, far away from the pronounced LiOH effect and nearly as good as CsOH with respect to the tendency to induce accelerated corrosion.

4.2 Mechanistic aspects

The weight gain results clearly show two distinct regions of alkali induced corrosion of zirconium alloys: a pre transition region with minor but significant effects of enhanced corrosion in different environments and a region of accelerated corrosion. Both phenomena may be but are not necessarily governed by the same corrosion mechanism. The incorporation and substitution of Zr in the dense growing zirconium oxide was suggested by Hillner and Chirigos [4] in their solid solution model for an increased number of anion vacancies which enhance the O^{2-} defects and lead to higher corrosion rates by an increased anion conductivity. This incorporation into the zirconium oxide lattice is highly dependent on the radius of the cation for substitution into the host lattice. If we compare the ion radii for the different alkali cations to the radius of Zr^{4+} (72 pm) one can

easily see that only Li^+ has an comparable size (see Table 1). The tendency for incorporation should significantly decrease if Li is changed to Na to Cs with their larger ionic radii. If there is a correlation between corrosion and cation substitution in the oxide, this can be obseved in the enhanced weight gains obtained under equimolar alkali hydroxide conditions in the region prior to accelerated corrosion. The diagrams presented in Fig. 8 and 9 clearly show this dependency. If we plot the measured weight gains obtained in 4.5 mmol solutions versus the inverse radius of the incorporated cation, as has been done in Fig. 14 for group A and Fig. 15 for group B materials (excluding the RbOH data), a linear relation is obtained especially for the 90 day exposure data. The validity of this relation points to a radius dependent conductivity in the zirconium oxide. The same plot performed with the data at higher alkali concentrations shows a non linear dependency. This can be understood

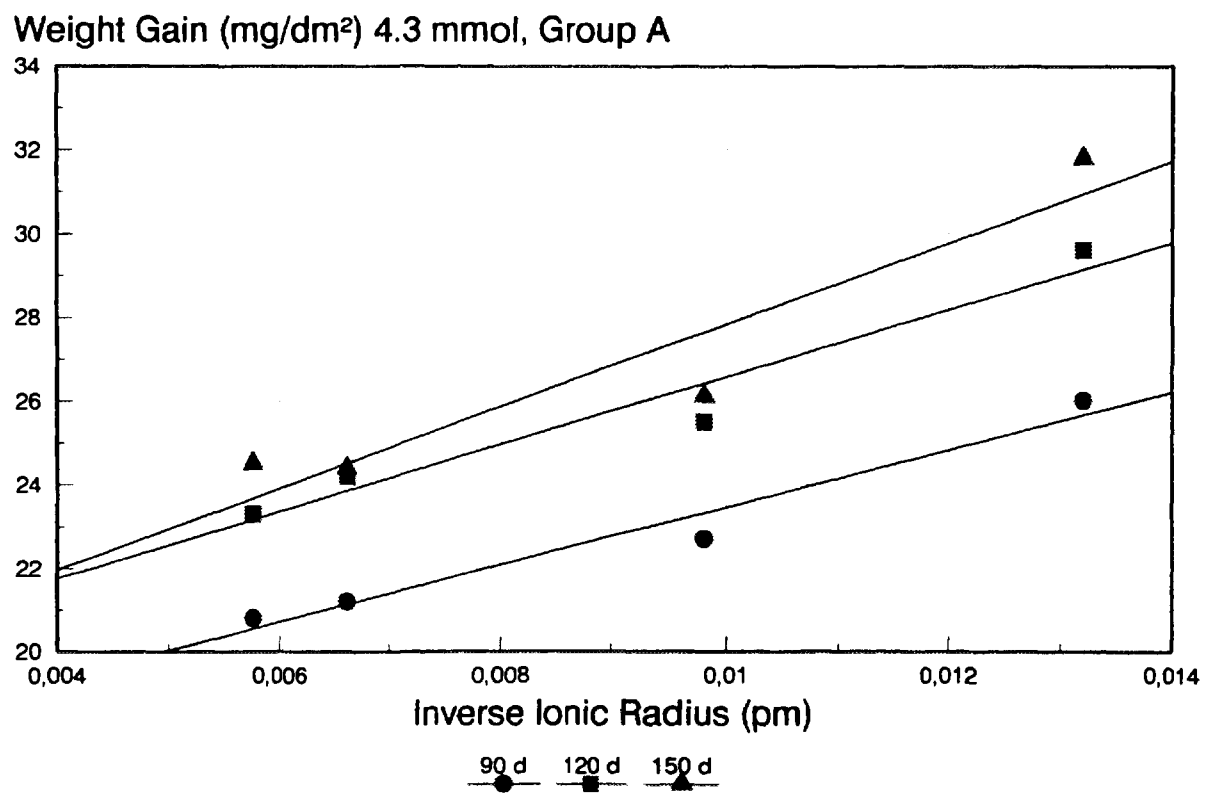

Fig. 14 Weight gain of group A material vs. inverse ion radii for different alkali hydroxide cations.

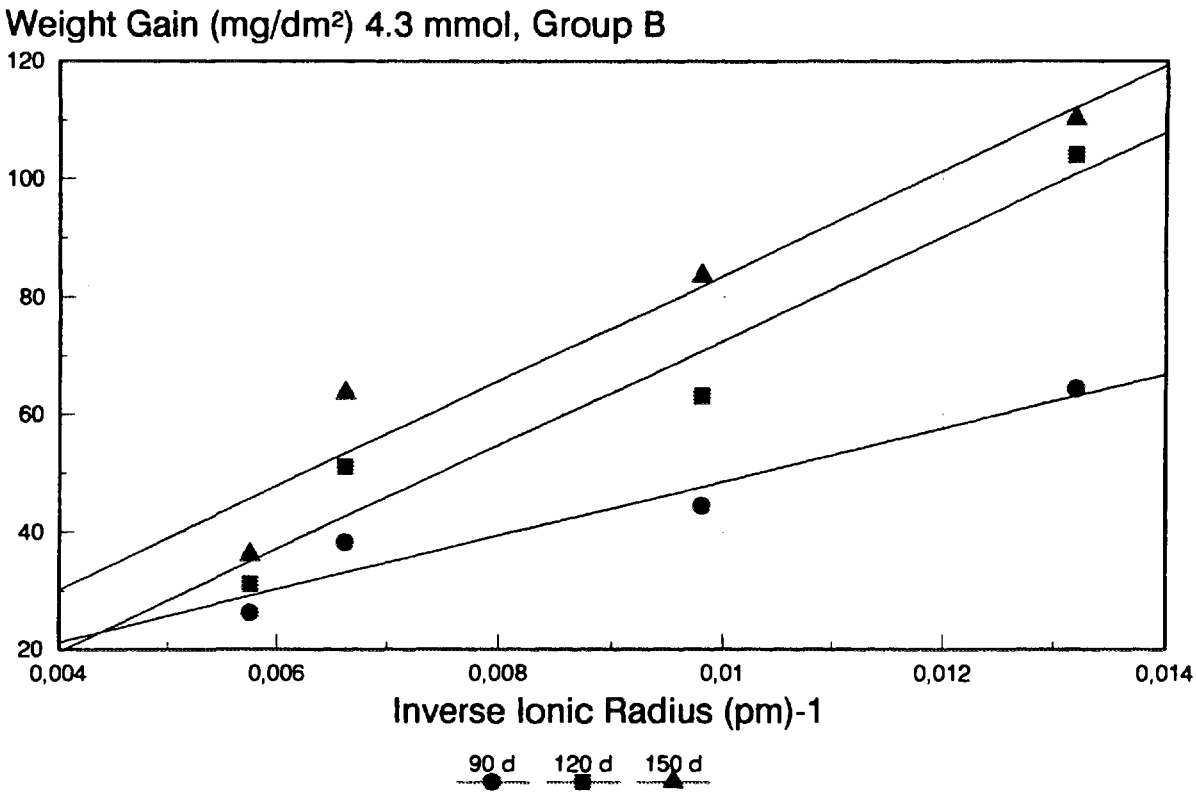

Fig. 15 Weight gain of group B material vs. inverse ion radii for different alkali hydroxide cations.

due to the fact that under these concentrations accelerated corrosion occurs for some of the materials in LiOH which can not be understood by ion substitution in the dense oxide. This accelerated corrosion phenomenon obviously is not governed by a substitutional effect. Probably crystal growth effects like nucleation and recrystallization and the development of porous structures may be influenced by the different environments. Whether the cation or the anion is responsible for this crystal growth effect is not yet answered. But this question may be solved by tests with prolonged exposure times under higher molar concentrations of the alkali hydroxides than applied in this study.

5. CONCLUSION

From the results presented in this study we draw the following conclusions:

1. From the experiments performed under equimolar conditions for the group-I-alkali hydroxides, the cation could be identified as the responsible species for zirconium alloy corrosion in alkalized water

2. The radius of the cation governs the corrosion behavior in the pre accelerated region of zircaloy corrosion. Incorporation of alkali cations into the zirconium oxide lattice is probably the mechanism which allows the corrosion enhancement for Li and Na and the significant lower effect for the other bases.

3. Nb containing alloys show lower corrosion resistance than alloys from the Zr-Sn-TRM system in all alkali solutions. Both types of alloys corrode significantly more in LiOH and NaOH than in the other alkali environments. Lowest corrosive aggressiveness has been found for CsOH followed by KOH.

4. Concluding from the corrosion behavior in the different alkali environments and taking into account the tendency to promote accelerated corrosion, CsOH and KOH are possible alternate alkali for PWR application.

REFERENCES

[1] Billot, Ph., Beslu, P., Giordano, A. and Thomazet, ASTM STP 1023, pp.165-184.

[2] Kass, S. , Corrosion , Vol. 25, No. 1, 1969, pp. 30-46.

[3] Murgatroyd, R. A. and Winton, J. Journal of Nuclear Materials, Vol 23, 1967, pp. 249-256.

[4] Hillner, E. and Chirigos J. N., Bettis Atomic Power Laboratory, Report WAPD-TM-307 (1962).

[5] McDonald, S.G., Sabol, G. P. and Sheppard, K. D., ASTM-STP 824 (1984), p. 519.

[6] Andrako, A. M. and Fisch, H. A., Knolls Atomic Power Laboratory, KAPL-2000-19.

[7] Coriou, H., Grall, L., Meunier, J. Pelras, M. and Willermoz, H., Journal of Nuclear Materials, Vol. 7, 1962, pp. 320-327.

[8] Perkins, R. A. and Bush, R., ASTM-STP 1132, 1991, pp. 595-612.

[9] Garzarolli, F. , Pohlmeyer J., Trapp-Pritsching, S. and Weidinger, H. G., Proc. IAEA Tech. Comm. on Fundamental Aspects of Corrosion..., Portland 1989, WGFPT/34, p. 34.

[10] Bramwell, I. L., Parsons, P. D. and Tice, D. R., ASTM-STP 1132, pp. 628-642.

[11] Ramasubramanian, N., Precoanin, N. and Ling, V.C., ASTM-STP 1023, pp. 187-201.

[12] Garzarolli, F., Seidel, H. Tricot, R. and Gros, J. P., ASTM-STP 1132, pp. 395-415.

[13] Ramasubramanian, N., Balakrishnan, P. V. Preprint of a paper presented at the 10th International Conferenceon Zirconium in the Nuclear Industry, Baltimore 1993.

[14] Garzarolli, F. and Holzer, R. Nucl. Energy, 31, 1992, pp. 65-85.

[15] Cox, B. and Chenguang, W. Journal of Nucl. Mat., 199, 1993, pp. 272-284.

[16] Rosenfeld, I. L., Olbrownikow, J. P. and Szudarikowa, A. A. IAEA Meeting on Corrosion of Reactor Materials, Salzburg, June 1962.

[17] McCullough, J. D. and Trueblood, K. N., Acta Cryst., 12, 1959, p. 507.